RESEARCH PAPER

Bioengineered 6:3, 141–148; May/June 2015; © 2015 Taylor & Francis Group, LLC

Structural studies on Laz, a promiscuous anticancer Neisserial protein

Wataru Hashimoto[1], Akihito Ochiai[1], Chang Soo Hong[2], Kousaku Murata[1], and Ananda M Chakrabarty[2,*]

[1]Laboratory of Basic and Applied Molecular Biotechnology; Graduate School of Agriculture; Kyoto University; Uji, Kyoto, Japan; [2]Department of Microbiology & Immunology; University of Illinois College of Medicine; Chicago, IL USA

Keywords: azurin, disorder, H.8 epitope, laz, neisseria, X-ray crystallography

Azurin and Laz (lipidated azurin) are 2 bacterial proteins with anticancer, anti-viral and anti-parasitic activities. Azurin, isolated from the bacterium *Pseudomonas aeruginosa,* termed Paz, demonstrates anticancer activity against a range of cancers but not against brain tumors. In contrast, Laz is produced by members of *Gonococci/Meningococci*, including *Neisseria meningitides* which can cross the blood-brain barrier to infect brain meninges. It has been previously reported that Laz has an additional 39 amino acid moiety, called an H.8 epitope, in the N-terminal part of the azurin moiety that allows Laz to cross the entry barrier to brain tumors such as glioblastomas. Exactly, how the H.8 epitope helps the azurin moiety of Laz to cross the entry barriers to attack glioblastoma cells is unknown. In this paper, we describe the structural features of the H.8 moiety in Laz using X-ray crystallography and demonstrate that while the azurin moiety of Laz adopts a β-sandwich fold with 2 β-sheets arranged in the Greek key motif, the H.8 epitope was present as a disordered structure outside the Greek key motif. Structures of Paz and H.8 epitope-deficient Laz are well superimposed. The structural flexibility of the H.8 motif in Laz explains the extracellular location of Laz in Neisseria where it can bind the key components of brain tumor cells to disrupt their tight junctions and allow entry of Laz inside the tumors to exert cytotoxicity.

Introduction

Azurin, a blue copper-containing protein belonging to the cupredoxin superfamily, is localized in the periplasm of gram-negative bacteria and is involved in electron transport during respiration.[1] Although structural and functional characteristics of bacterial azurin as a redox protein have been well documented,[2] we found the following additional function of the protein: clinical isolates of *Pseudomonas aeruginosa* secrete azurin extracellularly in response to the presence of various human cancer cells (e.g., melanoma and breast cancer cells).[3] Azurin exhibits significant cytotoxicity against cancer cells, while little cytotoxicity is observed against normal cells.[4] The protein can preferentially enter cancer cells and bind to the tumor suppressor protein p53.[5] The complex formed by azurin and p53 as well as its electron transfer partner cytochrome *c* induces apoptosis in cancer cells through cell cycle arrest at the G1 phase or caspase-mediated mitochondrial cytochrome *c* release.[6,7] Azurin is therefore expected to be a potential drug for cancer therapy.[8,9]

The precursor form of azurin (148 residues) produced by *P. aeruginosa* is converted to a mature form (Paz, 128 residues) through the release of a signal peptide (20 residues) across the inner membrane (**Fig. 1**).[10] Site-directed mutagenesis and deletion mutations indicate that the presence of a copper ion and redox activity was not essential for the cytotoxicity of Paz.[11] The internal sequence of Paz (residue nos. 50–77 in the mature form, termed p28) functions as a putative protein transduction domain responsible for azurin's penetration into cancer cells[12] through endocytotic and nonendocytotic mechanisms.[13] Based on crystal structures, bacterial azurins show structural similarity to ephrinB2, a ligand for the receptor tyrosine kinase EphB2.[14,15] Cell signaling through Eph/ephrin is involved in cancer progression.[14,15] The chemically synthesized C-terminal domain of Paz (residue nos. 96–113 in the mature form), which is similar to ephrinB2 at the GH loop region responsible for receptor binding,[15] inhibits the growth of various cancer cells.[14] Indeed, it has been shown that azurin represses ephrinB2-mediated autophosphorlyation of the EphB2 tyrosine residue, thereby interfering with upstream cell signaling and contributing to cancer cell growth inhibition.[14]

In addition to azurin, rusticyanin, another bacterial cupredoxin, causes apoptosis in human cancer cells.[16] Neisserial azurin-like protein, a "lipobox"-dependent lipid-modified azurin (Laz) bound to the outer membrane,[17] also enters brain tumors such as glioblastomas and exhibits significant toxicity against the cancer cells,[18] suggesting that Laz must cross the entry barrier to reach brain tumor cells. Laz includes a 39-amino acid residue region called the H.8 epitope at the N terminus prior to the azurin domain. In our previous studies with Laz, the H.8 epitope of the protein, but not its lipidation, was demonstrated to be

*Correspondence to: Ananda M Chakrabarty; Email: pseudomo@uic.edu
Submitted: 01/15/2015; Revised: 02/15/2015; Accepted: 02/19/2015
http://dx.doi.org/10.1080/21655979.2015.1022303

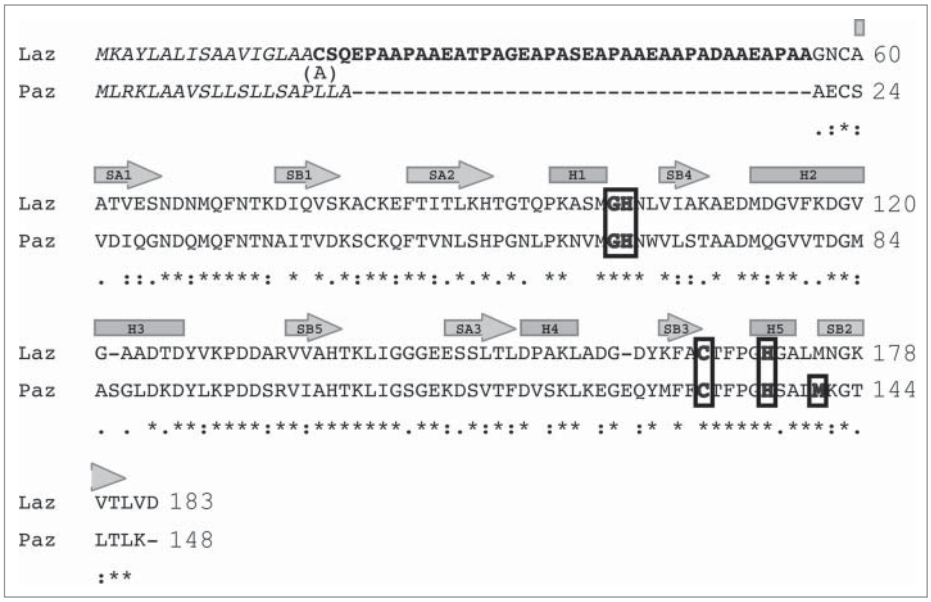

Figure 1. Amino acid sequence alignment of Laz and Paz using the CLUSTALW program (http://clustalw.genome.ad.jp/). Laz, *Neisseria gonorrhoeae* azurin; Paz, *Pesudomonas aeruginosa* azurin. Identical and similar amino acid residues in Laz and Paz are denoted by asterisks and dots, respectively. Letters in italic and bold indicate the signal peptide and H.8 epitope, respectively. The amino acid residues responsible for binding to the metal ion are boxed. The regions corresponding to cylinders and arrows represent α-helices and β-strands, respectively. The H.8 epitope is intrinsically disordered. Laz used in this study has Ala18 instead of Cys18.

essential for disrupting the entry barrier to provide access to brain tumor cells.[18] To obtain clues on the entry of Laz into brain tumor cells, we determined the structure of Laz by X-ray crystallography and our findings are described herein.

Results

Comparison of primary structure between Laz and Paz

Laz consists of 183 amino acid residues with a molecular weight of 18532 (**Fig. 1**).[17] Similar to other bacterial outer membrane-bound lipoproteins, Laz includes a conserved 4-amino acid sequence termed lipobox [LVI][ASTVI][GAS]C at the N terminus.[19,20] The thiol group of the cysteine residue in the lipobox accepts diacylglycerol from phosphatidylglycerol through the action of transferase Lgt, and the resultant lipid-modified proteins are processed by signal peptidase II. The N-terminal 17 amino acid residues are therefore considered to function as a sorting signal to the outer membrane. On the other hand, Paz is known to be a protein secreted through processing of a 20-residue signal peptide by signal peptidase I.

After processing by signal peptidase II, mature Laz consists of 166 residues with the N-terminal 39-residue sequence designated as the H.8 epitope (**Fig. 1**). This epitope includes a repeated sequence of 5 amino acid residues and exhibits a significantly low isoelectric point (pI 3.4). A substantial sequence identity (56%) exists in the azurin domain between Laz and Paz. Although the crystal structure of Paz has already been solved, no information is available on the structure of Laz, especially of the H.8 epitope. Thus, X-ray crystallography of Laz was performed to clarify the structure–function relationship of the H.8 epitope involved in disrupting the entry barrier to brain tumor cells.

Purification and characterization of Laz

Lipidation is known to hinder crystallization of lipoproteins. Thus, the Laz mutant with a pectate lyase B (*pelB*) signal peptide instead of the native lipobox peptide was purified and characterized because this mutant can also enter glioblastoma cells and exhibit cytotoxicity.[18] In the mutant, the signal peptide was fused to the H.8 epitope with the N-terminal cysteine residue (Cys18) substituted with alanine (Ala18) to avoid lipidation (**Fig. 1**). Laz purified from the recombinant *E. coli* cells showed a single protein band of 22 kDa on the SDS-PAGE gel (**Fig. 2**, inset). Positive-mode matrix-assisted laser desorption/ionization time-of-flight mass spectrometry demonstrated that the molecular weight of the purified protein was 16832 (**Fig. 2**). The signal at *m/z* 8425 was considered to be derived from the sample in the divalent ion form. The N-terminal amino acid sequence of the purified Laz was determined to be NH_2–ASQEP corresponding to[18]ASQEP,[22] indicating that the mature protein, formed after cleavage of the signal peptide, consists of 166 amino acid residues with a theoretical molecular weight of 16841 which is in good agreement with that determined by mass spectrometry (16832). The difference in molecular weight between SDS-PAGE and mass spectrometry is possibly due to the significantly low pI of the H.8 epitope. Inductively coupled plasma atomic emission spectrometry analysis revealed that the protein contained metal ions such as zinc and copper. The content of zinc ion was fold10- higher than that of copper ion.

Structure determination

Stick-shaped crystals of Laz were found in a droplet consisting of 1.5 M ammonium sulfate, 0.1 M Tris-HCl (pH 8.5), and 20% glycerol (**Fig. 3**, inset). Diffraction images of the crystal were collected at up to 1.90 Å resolution (**Fig. 3**). The structure of Laz was solved by molecular replacement, using Paz as a reference model. Statistics for data collection and structure refinement are shown in**Table 1**. The N-terminal sequence (40 amino acid residues, Ala18–Gly57) closely corresponding to the H.8 epitope could not be assigned in the $2F_o$-F_c map. The refined model in an asymmetric unit consisted of 2 identical monomers (126 amino acid residues, Asn58–Asp183 × 2) termed molecules A and B with 161 water molecules, 2 metal ions, 2 sulfate ions, and 2 glycerol molecules; root-mean-square deviation (rmsd) between molecules A and B was calculated as 0.191 Å for all residues (126

Cα atoms), indicating that the structures of molecules A and B are basically identical to each other. On the basis of theoretical curves in the plot calculated according to Luzzati,[21] the absolute positional error was estimated to be 0.214 Å at 1.90 Å resolution. Ramachandran plot analysis[22] in which the stereochemical correctness of the backbone structure is indicated by (φ, ψ) torsion angles showed that 93.1% of nonglycine residues lie within the most favored regions and 6.9% of nonglycine residues lie in the additionally allowed regions.

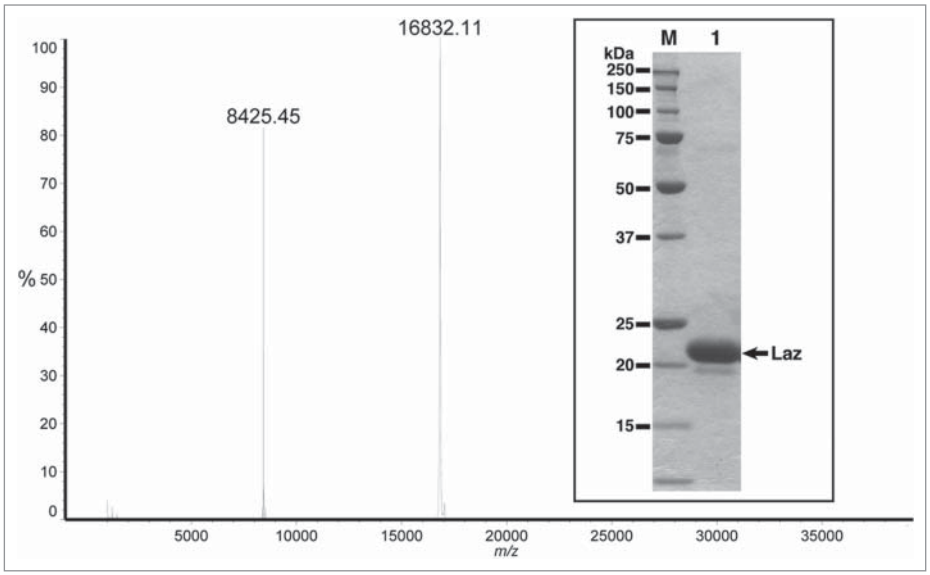

Figure 2. Molecular mass of Laz from positive-mode matrix-assisted laser desorption/ionization time-of-flight mass spectrometry. Inset, SDS-PAGE profile, lane M, molecular weight standards; lane 1, the purified Laz (10 μg).

Overall structure

The overall structure (**Fig. 4A**) and topology of secondary structure elements (**Fig. 4B**) indicate that the H.8 epitope-deficient Laz (C-terminal domain of Laz, Laz-C) adopts a β-sandwich fold as a basic scaffold. Five additional α-helices (H1, residues 96–101; H2, 111–120; H3, 121–126; H4, 153–158; and H5, 170–174) are included in the domain. The β-sandwich fold consists of 2 β-sheets arranged in the Greek key motif. One sheet (SA) is composed of 3 strands (SA1, 60–65; SA2, 85–91; and SA3, 147–152) and the other (SB) has 5 strands (SB1, 75–79; SB2, 176–182; SB3, 162–165; SB4, 105–108; and SB5, 135–138).

Structural homologs of Laz-C were searched in Protein Data Bank (PDB) using the DALI program.[23] Bacterial azurin proteins were found to exhibit significant structural homology with Laz-C (**Table 2**). The overall structure of Laz-C is most similar to that of *Alcaligenes xylosoxidans* azurin (PDB code, 1RKR; $Z =$ 24.7) with rmsd of 1.0 Å for 126 Cα. Laz-C is also structurally similar to Paz ($Z = 24.5$). Superimposition of the crystal structures of Laz-C and Paz (PDB code, 1AG0) is shown in **Fig. 5A**. Because a large number of bacterial azurins and plant plastocyanins with the Greek key motif are categorized into the plastocyanin/azurin-like family in the cupredoxin superfamily on the SCOP database (http://scop.mrc-lmb.cam.ac.uk/scop/), Laz-C is considered to be structurally classified into this family.

Metal-binding site

A density map for metal ions was observed in each protein molecule, suggesting that Laz contained one molecule of metal ion per protein molecule. Although inductively coupled plasma atomic emission spectrometry showed that 2 ions such as zinc and copper are included in Laz, the protein was suggested to contain a zinc or copper ion. Based on the content of metal ions, Laz used in this study is considered to incorporate a zinc rather than a copper ion. This is possibly due to an insufficient supply of copper ions during culturing of the bacteria, purification of the protein, or both. The four atoms, O of Gly101, Nδ of His102, Sγ of Cys166, and Nδ of His171, are coordinated to the zinc ion, and the coordination geometry comprises a distorted tetrahedron (**Fig. 5B**, left). The distance between the zinc ion and these atoms ranges from 1.94 to 2.30 Å (average, 2.15 Å).

The copper ion in Paz (Cu-Paz) is known to be bound to 5 atoms, O of Gly65, Nδ of His66, Sγ of Cys132, Nδ of His137, and Sδ of Met141 (**Fig. 5B**, right, purple).[24] These 5 residues (G/H/C/H/M) involved in binding to the copper ion are also completely conserved in Laz (**Fig. 1**), although Met175 in Laz-C is located slightly

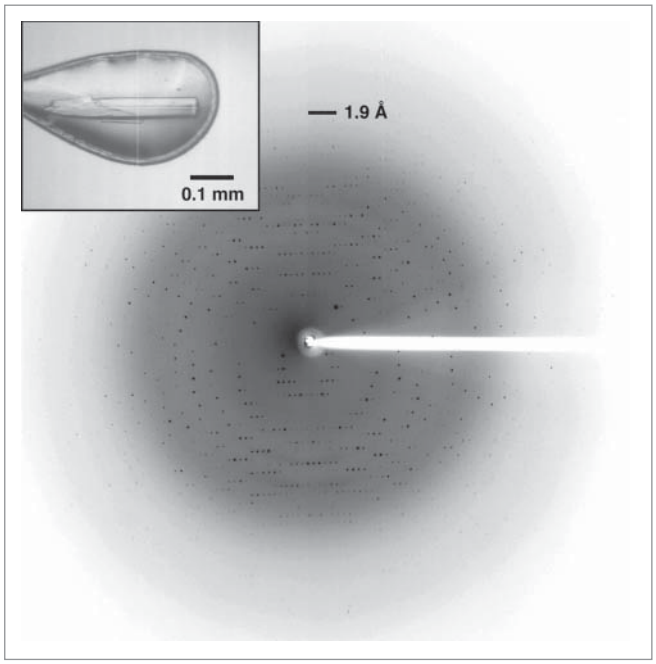

Figure 3. X-ray crystallography of Laz. Diffraction image of the Laz crystal (inset) collected at up to 1.90 Å resolution.

Table 1. Data collection and refinement statistics

Space group	$P6_5$
Unit cell parameters (Å)	$a = b = 77.5$, $c = 94.6$
Data collection	
Wavelength (Å)	1.0000
Resolution limit (Å)	50.0–1.90 (1.97–1.90)[a]
Total reflections	76,372
Unique reflections	25,438
Redundancy	3.1 (2.9)
Completeness (%)	96.9 (92.8)
I/Sigma (I)	9.6 (1.54)
R_{merge} (%)	6.0 (39.7)
Refinement	
Final model	252 (126 × 2) amino acid residues, 161 water molecules, 2 zinc ions, 2 sulfate ions, 2 glycerol molecules
Resolution limit (Å)	31.6–1.90 (1.95–1.90)
Used reflections	23,363 (1,637)
Completeness (%)	97.0 (92.5)
Average *B* factor (Å^2)	
Protein (molecule A, B)	23.8, 24.6
Water molecules	36.0
Copper ion	20.2
Sulfate ion	33.7
Glycerol molecules	33.0
R factor (%)	19.3 (25.5)
R_{free} (%)	22.5 (29.5)
Root-mean-square deviations	
Bond (Å)	0.008
Angle (°)	1.15
Ramachandran plot (%)	
Most favored regions	93.1
Additional allowed regions	6.9
Generously allowed regions	0.0

[a]Data on highest shells are given in parentheses.

farther from the zinc ion (3.50 Å) (**Fig. 5B**, left). Among a large number of azurin-like crystal structures determined to date, a zinc ion-bound Paz (Zn-Paz) expressed in recombinant *E. coli* cells has been isolated and structurally characterized.[25] In the crystal structure of Zn-Paz (PDB code, 1E67), the distance between the zinc ion and Sδ of Met141 is 3.31 Å (**Fig. 5B**, right, blue), while the corresponding distance is 2.97 Å in Cu-Paz (PDB code, 3AZU) (**Fig. 5B**, right, purple), indicating that Laz-C is structurally similar to Zn-Paz.

Table 2. Structure-based homology with Laz

Z score	Description	rmsd[a]	Lali[b]	PDB ID
24.7	*Alcaligenes xylosoxidans* azurin	1.0	126	1RKR
24.7	*Pseudomonas putida* azurin	0.8	125	1NWP
24.5	*Alcaligenes denitrificans* azurin	1.0	126	1AZB
24.5	*Pseudomonas aeruginosa* azurin	0.9	125	1R1C

[a]Root-mean-square deviations.
[b]Total number of equivalence residues.

Discussion

Because of disorder, the structure of the H.8 epitope could not be determined. Recently, natively unfolded or intrinsically disordered proteins (IDPs) or regions have been found mainly in eukaryotic cells.[26,27] In addition, the sigma factor inhibitor FlgM in bacteria has been identified as an IDP.[28] A large number of IDPs are classified as a superfamily of macromolecule (DNA, RNA, or protein)-associated proteins such as transcriptional factors, RNA-binding proteins, and cell cycle regulators.[27] A typical IDP is the transcriptional factor leucine zipper protein GCN4.[29] The basic DNA-binding region in GCN4 is unfolded in the absence of DNA, while a helical structure is inducibly formed in the region of DNA binding. This is called the coupled binding and folding process.[26]

Through bioinformatics approaches, 5 common features of IDPs are postulated:[26,27] (i) Short sequences are repeated in IDPs. (ii) Little sequence homology is observed in disordered regions among IDPs. (iii) Disordered regions are located at the N or C terminus of IDPs. (iv) IDPs are primarily produced by eukaryotes. (v) IDPs are frequently localized in the nucleus and rarely in mitochondria. In case of Laz, the N-terminal H.8 epitope with a 5 residue-repeated sequence (AAEAP, a typical but somewhat variable sequence) is attached to the azurin domain (**Fig. 1**). No proteins or peptides were found to be homologous to the H.8 epitope in the protein databases. Several programs for identification of intrinsically disordered regions in IDPs are available on the web. The H.8 epitope of Laz was predicted to be intrinsically disordered by all the typical programs, PONDR-FIT,[30] DISOPRED 2,[31] and DisEMBL[32] (**Figs. 1** and **6**). Although the target molecules that bind to Laz have not been identified in the entry barrier to brain tumors, the intrinsically disordered H.8 epitope may inducibly fold into a rigid structure by binding to target molecules.

Why is the H.8 epitope of Laz intrinsically disordered rather than being integrated with the folded region of Laz-C? It should be emphasized that the H.8 epitope of Laz seems to have 2 major functions in which a loosely associated H.8 epitope may be required. First, the H.8 epitope has been shown to be involved in facilitating the entry of Laz-C (the 127 amino acid azurin moiety) into glioblastomas[18] as well as its passage through the blood–brain barrier.[33] Thus, the presence of the H.8 epitope allows the Laz-C moiety to enter glioblastoma or other brain tumors when *Neisseria* such as *N. meningitides* are present in the brain meninges. Because *P. aeruginosa* does not normally cause infections in the brain, it has no particular need to equip its anticancer weapon Paz with a blood–brain barrier-crossing capability. The other hypothetical function of the H.8 epitope is to allow *N. meningitides* to protect its weapon Laz-C from being attacked by the immune system following the release of Laz-C from the bacterial cells for entry into the tumor. Interestingly, the H.8 epitope has been shown[34] to induce formation of blocking antibodies that bind complements or other antibodies generated by the host to remove the invading bacteria thereby inactivating the host-generated antibodies. Such induction of blocking antibodies by the H.8 epitope is believed to prevent

complement-mediated bactericidal action and provide a survival advantage to group B *meningococci*.[34] It is, however, equally possible that such blocking antibodies protect Laz from immune attack when released for entry into brain tumors. Normally, azurin (Paz) demonstrates low immunogenicity because of its structural similarity with immunoglobulins. Both azurin and immunoglobulins, while having low sequence identity, demonstrate structural features with β-sandwich packing.[8] Both these proteins exhibit tyrosine residues in a motif called the "tyrosine corner," which plays a significant role in the structural stability and folding of the Greek key β-barrel structure exhibited by azurin and immunoglobulins.[8] This low immunogenicity of azurin (Laz-C) is further enhanced by the presence of the intrinsically disordered H.8 epitope that elicits blocking antibodies to protect Laz from immune attack.

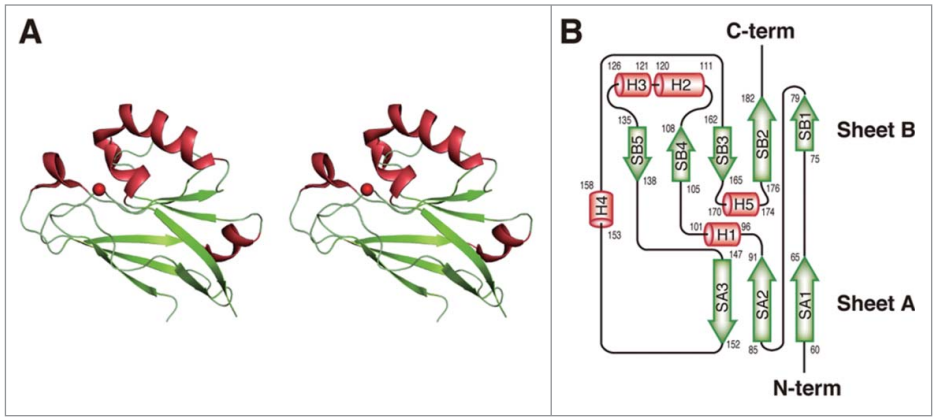

Figure 4. Structure of Laz. (**A**) Overall structure (stereo diagram). (**B**) Topology diagram. α-Helices are shown as orange cylinders and β-strands as green arrows. The metal ion is depicted by a red ball.

In conclusion, this is the first report on the structure of Neisserial azurin (Laz), which is cytotoxic to brain and other tumor cells. Laz is composed of an N-terminal intrinsically disordered H.8 epitope and a rigid azurin domain with the Greek key motif. In contrast, the *P. aeruginosa* azurin Paz, which lacks the H.8 epitope, is deficient in the ability to enter brain tumor cells and consequently demonstrates significantly lower cytotoxicity against such cells.[18,33] It should be noted, however, that as mentioned earlier, Paz, unlike Laz, is deficient in entry in glioblastoma cells, while H.8-Paz, where the H.8 epitope was cloned in the N-terminal of Paz, had significant cytotoxicity against glioblastoma cells, confirming the presence of the H.8 epitope as critical for entry in brain tumors. It should also be noted that Paz, Laz and H.8-Paz had not only anticancer activity, but strong anti-viral activity against the AIDS-causing HIV-1 virus and strong anti-parasitic activity against parasites such as the malarial parasite *Plasmodium falciparum*[35] and the toxoplasmosis-causing parasite *Toxoplasma gondii*.[36] The potential clinical importance of such bacterial proteins as Paz and Laz is reflected in the fact that a 28 amino acid peptide fragment from azurin (azurin 50–77), termed p28, has shown very little toxicity in 15 stage IV cancer patients in a phase I clinical trial, but significant beneficial effect including partial and complete regression of the drug-resistant tumors in several patients.[37] Another phase I trial with p28, currently in progress in pediatric brain tumor patients in 11 hospitals in the US

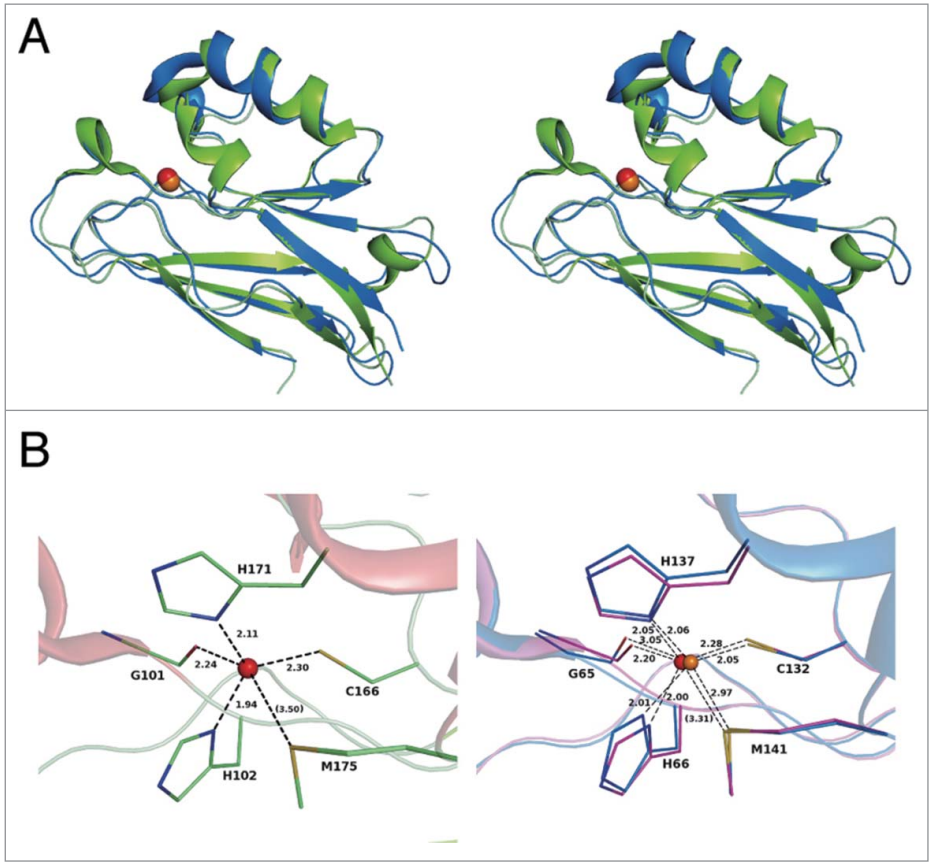

Figure 5. Structural comparison. (**A**) Superimposition of the overall structures of Laz-C (green) and Paz (blue) (PDB code, 3AZU). (**B**) Metal-binding site. Left, Laz (carbon, green; nitrogen, blue; oxygen, red; and sulfur, yellow); right, superimposition of copper (blue)- and zinc (purple)-binding Paz proteins. Balls colored red and orange indicate the zinc and copper ions, respectively.

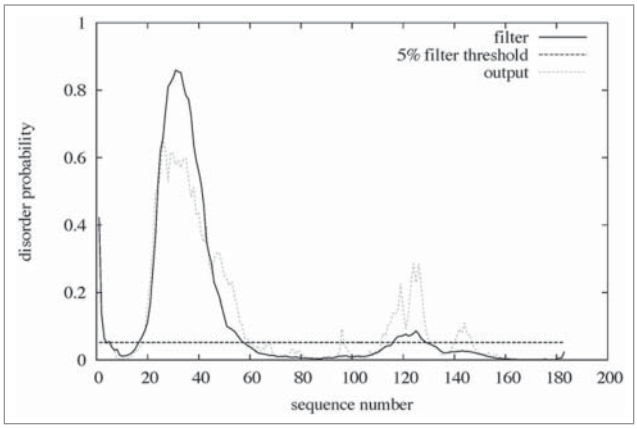

Figure 6. Disordered region in Laz. The amino acid sequence of Laz (183 residues) was analyzed by the disorder prediction program DISOPRED 2 (http://bioinf.cs.ucl.ac.uk/disopred/). Residues (20–58) corresponding to the H.8 epitope were identified as a disordered region.

(http://clinicaltrials.gov/ct2/show/NCT01975116) for more than a year and 3 months appears to indicate that p28, even lacking the H.8 epitope but with a smaller size than azurin, may be able to enter the brain tumors to allow their regression.

Materials and Methods

Microorganisms and culture conditions

Escherichia coli strain BL21(DE3) (Novagen) was used as a host for expression of *Neisseria gonorrhoeae* Laz. For expression in *E. coli*, cells were aerobically precultured at 30°C in Luria–Bertani medium[38] supplemented with sodium ampicillin (0.1 mg/ml). When the turbidity reached approximately 0.5 at 600 nm, isopropyl-β-D-thiogalactopyranoside was added to the culture (0.1 mM) and the cells were further cultured for 44 h at 16°C.

Purification

Unless otherwise specified, all operations were performed at 0–4°C. *E. coli* cells harboring pET25b-lca[18] were grown in 6 l of LB medium (1.5 l/flask), collected by centrifugation (6000 ×*g* for 5 min at 4°C), washed with 20 mM Tris-HCl (pH 7.5), and subsequently resuspended in the same buffer. The cells were ultrasonically disrupted (Insonator Model 201M; Kubota) at 9 kHz for 20 min at 0°C, and the clear solution obtained on centrifugation at 20000 ×*g* and 4°C for 20 min was used as the cell extract. The extract was applied to a DEAE-Toyopearl 650 M (Tosoh) column (2.6 cm × 10 cm) previously equilibrated with 20 mM Tris-HCl (pH 7.5). The absorbed proteins were eluted with a linear gradient of NaCl (0–1 M) in 20 mM Tris-HCl (pH 7.5, 300 ml), and a 6.6-ml fraction was collected every 7 min. The fractions containing Laz, eluted with 0.2–0.3 M NaCl, were combined and saturated with ammonium sulfate (30%). The Laz solution was then applied to a Butyl-Toyopearl 650M (Tosoh) column (2.6 cm × 10 cm) previously equilibrated with 20 mM Tris-HCl (pH 7.5) containing 30% saturated ammonium sulfate. The absorbed proteins were eluted with a linear gradient of saturated ammonium sulfate (30–0%, 300 ml), and a 6.6-ml fraction was collected every 10 min. The Laz fractions, eluted with 20–10% saturated ammonium sulfate, were combined and dialyzed for 3 h against 20 mM Tris-HCl (pH 7.5). The dialysate was applied to a SuperQ-Toyopearl 650S (Tosoh) column (1 cm × 10 cm) previously equilibrated with 20 mM Tris-HCl (pH 7.5). The absorbed proteins were eluted with a linear gradient of NaCl (0–0.5 M) in 20 mM Tris-HCl (pH 7.5, 30 ml), and a 1-ml fraction was collected every 1 min. The Laz fractions, eluted with 0.2–0.25 M NaCl, were combined and applied to a HiLoad 16/60 Superdex 75 pg (GE healthcare) column (1.6 cm × 60 cm) previously equilibrated with 20 mM Tris-HCl (pH 7.5) containing 0.15 M NaCl. Laz was eluted with the same buffer (120 ml), and a 2-ml fraction was collected every 2 min. The Laz fractions were combined and dialyzed for 3 h against 20 mM Tris-HCl (pH 7.5). The dialysate was used as the purified Laz. The homogeneity of the purified protein was confirmed by SDS-PAGE.[39] The protein content was determined by measuring the absorbance at 280 nm using a cuvette with a path length of 1 cm, assuming that $E_{280} = 0.177$ (Laz) corresponds to 1 mg/ml.

Analytical methods

The N-terminal amino acid sequence of Laz was determined by the Edman degradation method using a Procise 492 protein sequencer (Applied Biosystems). The molecular weight of Laz was determined using a matrix-assisted laser desorption/ionization time-of-flight mass spectrometer (AXIMA Performance; Shimadzu); sinapinic acid was used as the matrix. Metal ions included in Laz were examined using an inductively coupled plasma atomic emission spectrometer (ICPS-8100; Shimadzu).

Crystallization and X-ray diffraction

Laz (98 mg/ml) was crystallized at 20°C using the sitting drop vapor diffusion method. The mother liquor consisting of 1.5 M ammonium sulfate, 0.1 M Tris-HCl (pH 8.5), and 20% glycerol (100 μl) was used as a reservoir solution, and 1 μl of the Laz solution was mixed with 1 μl of the reservoir solution to form the drop. The Laz crystal was removed from the drop solution using a mounted nylon loop (Hampton Research) and then placed directly into a cold nitrogen gas stream at −173°C. X-ray diffraction images of the crystal were collected at −173°C under a nitrogen gas stream using a Jupiter 210 charge-coupled device detector and synchrotron radiation at the BL-38B1 station of SPring-8 (Japan). The diffraction data for the native crystal were collected at 1.90 Å resolution and processed using the HKL2000 program package.[40] Data collection statistics from the crystal are summarized in **Table 1**.

Structure determination and refinement

The crystal structure of Laz was solved by molecular replacement using the Molrep program[41] in the CCP4 program package;[42] the Paz structure (PDB code, 1AG0) was used as a reference model. The Coot program[43] was used for manual modification of the initial model. Initial rigid body refinement and several rounds of restrained refinement against the dataset were

performed using the Refmac5 program.[44] Water molecules were incorporated where the difference in density exceeded 3.0σ above the mean and the $2F_o$-F_c map showed a density of over 1.0σ. At this stage, metal ions were included in the calculation and refinement continued until convergence at maximum resolution. Protein models were superimposed and their rmsd was determined using the LSQKAB program,[45] a part of CCP4. Final model quality was determined using the PROCHECK program.[46] Ribbon plots were prepared using the PyMOL program.[47] Coordinates used in this study were taken from PDB, Research Collaboratory for Structural Bioinformatics.[48]

Protein structure accession number

The atomic coordinates and structure factors (PDB code, 3AY2) of Laz have been deposited in PDB, Research Collaboratory for Structural Bioinformatics, Rutgers University, New Brunswick, NJ (http://www.rcsb.org/).

Disclosure of Potential Conflicts of Interest

No potential conflicts of interest were disclosed.

Acknowledgments

We thank Drs. S Baba and N Mizuno of the Japan Synchrotron Radiation Research Institute (JASRI) for their kind help in data collection. Diffraction data for crystals were collected at the BL-38B1 station of SPring-8 (Hyogo, Japan) with the approval of JASRI.

References

1. Lancaster KM, Farver O, Wherland S, Crane EJ, Richards JH, Pecht I, Gray HB. Electron transfer reactivity of type zero *Pseudomonas aeruginosa* azurin. J Am Chem Soc 2011; 133: 4865-73; PMID:21405124; http://dx.doi.org/10.1021/ja1093919
2. Savelieff MG, Lu Y. Cu(A) centers and their biosynthetic models in azurin. J Biol Inorg Chem 2010; 15: 461-83; PMID:20169379; http://dx.doi.org/10.1007/s00775-010-0625-2
3. Mahfouz M, Hashimoto W, Das Gupta TK, Chakrabarty AM. Bacterial proteins and CpG-rich extrachromosomal DNA in potential cancer therapy. Plasmid 2007; 57:4-17; PMID:17166586; http://dx.doi.org/10.1016/j.plasmid.2006.11.001
4. Punj V, Bhattacharyya S, Saint-Dic D, Vasu C, Cunningham EA, Graves J, Yamada T, Constantinou AI, Christov K, White B, et al. Bacterial cupredoxin azurin as an inducer of apoptosis and regression in human breast cancer. Oncogene 2004; 23: 2367-78; PMID:14981543; http://dx.doi.org/10.1038/sj.onc.1207376
5. Yamada T, Goto M, Punj V, Zaborina O, Kimbara K, Das Gupta TK, Chakrabarty AM. The bacterial redox protein azurin induces apoptosis in J774 macrophages through complex formation and stabilization of the tumor suppressor protein p53. Infect Immun 2002; 70: 7054-62; PMID:12438386; http://dx.doi.org/10.1128/IAI.70.12.7054-7062.2002
6. Hiraoka Y, Yamada T, Goto M, Das Gupta TK, Chakrabarty AM. Modulation of mammalian cell growth and death by prokaryotic and eukaryotic cytochrome *c*. Proc Natl Acad Sci USA 2004; 101:6427-32; PMID:15082831; http://dx.doi.org/10.1073/pnas.0401631101
7. Yamada T, Hiraoka Y, Ikehata M, Kimbara K, Avner BS, Das Gupta TK, Chakrabarty AM. Apoptosis or growth arrest: modulation of tumor suppressor p53s specificity by bacterial redox protein azurin. Proc Natl Acad Sci USA 2004; 101: 4770-5; PMID:15044691; http://dx.doi.org/10.1073/pnas.0400899101
8. Fialho AM, Stevens FJ, Das Gupta TK, Chakrabarty AM. Beyond host-pathogen interactions: microbial defense strategy in the host environment. Curr Opin Biotechnol 2007; 18:279-86; PMID:17451932; http://dx.doi.org/10.1016/j.copbio.2007.04.001
9. Chakrabarty AM, Bernardes N, Fialho AM. Bacterial proteins and peptides in cancer therapy: today and tomorrow. Bioengineered 2014; 5: 234-42; PMID:24875003; http://dx.doi.org/10.4161/bioe.29266
10. Arvidsson RH, Nordling M, Lundberg LG. The azurin gene from *Pseudomonas aeruginosa*. cloning and characterization. Eur J Biochem 1989; 179: 195-200; PMID:2537198; http://dx.doi.org/10.1111/j.1432-1033.1989.tb14540.x
11. Goto M, Yamada T, Kimbara K, Horner J, Newcomb M, Das Gupta TK, Chakrabarty AM. Induction of apoptosis in macrophages by *Pseudomonas aeruginosa* azurin: tumour-suppressor protein p53 and reactive oxygen species, but not redox activity, as critical elements in cytotoxicity. Mol Microbiol 2003; 47: 549-59; PMID:12519204; http://dx.doi.org/10.1046/j.1365-2958.2003.03317.x
12. Yamada T, Fialho AM, Punj V, Bratescu L, Das Gupta TK, Chakrabarty AM. Internalization of bacterial redox protein azurin in mammalian cells: entry domain and specificity. Cell Microbiol 2005; 7: 1418-31; PMID:16153242; http://dx.doi.org/10.1111/j.1462-5822.2005.00567.x
13. Taylor BN, Mehta RR, Yamada T, Lekmine F, Christov K, Chakrabarty AM, Green A, Bratescu L, Shilkaitis A, Beattie CW, et al. Noncationic peptides obtained from azurin preferentially enter cancer cells. Cancer Res 2009; 69: 537-46; PMID:19147567; http://dx.doi.org/10.1158/0008-5472.CAN-08-2932
14. Chaudhari A, Mahfouz M, Fialho AM, Yamada T, Granja AT, Zhu Y, Hashimoto W, Schlarb-Ridley B, Cho W, Das Gupta TK, et al. Cupredoxin-cancer interrelationship: azurin binding with EphB2, interference in EphB2 tyrosine phosphorylation, and inhibition of cancer growth. Biochemistry 2007; 46: 1799-810; PMID:17249693; http://dx.doi.org/10.1021/bi061661x
15. Chrencik JE, Brooun A, Recht MI, Nicola G, Davis LK, Abagyan R, Widmer H, Pasquale EB, Kuhn P. Three-dimensional structure of the EphB2 receptor in complex with an antagonistic peptide reveals a novel mode of inhibition. J Biol Chem 2007; 282: 36505-13; PMID:17897949; http://dx.doi.org/10.1074/jbc.M706340200
16. Yamada T, Hiraoka Y, Das Gupta TK, Chakrabarty AM. Rusticyanin, a bacterial electron transfer protein, causes G1 arrest in J774 and apoptosis in human cancer cells. Cell Cycle 2004; 3: 1182-7; PMID:15467448
17. Cannon JG. Conserved lipoproteins of pathogenic neisseria species bearing the H.8 epitope: lipid-modified azurin and H.8 outer membrane protein. Clin Microbiol Rev 1989; 2: S1-4; PMID:2470496
18. Hong CS, Yamada T, Hashimoto W, Fialho AM, Das Gupta TK, Chakrabarty AM. Disrupting the entry barrier and attacking brain tumors: the role of the neisseria H.8 epitope and the Laz protein. Cell Cycle 2006; 5: 1633-41; PMID:16861907; http://dx.doi.org/10.4161/cc.5.15.2991
19. Babu MM, Priya ML, Selvan AT, Madera M, Gough J, Aravind L, Sankaran K. A database of bacterial lipoproteins (DOLOP) with functional assignments to predicted lipoproteins. J Bacteriol 2006; 188: 2761-73; PMID:16585737; http://dx.doi.org/10.1128/JB.188.8.2761-2773.2006
20. Narita S, Tokuda H. An ABC transporter mediating the membrane detachment of bacterial lipoproteins depending on their sorting signals. FEBS Lett 2006; 580: 1164-70; PMID:16288742; http://dx.doi.org/10.1016/j.febslet.2005.10.038
21. Luzzati V. Traitement statistique des erreurs dans la determination des structures cristallines. Acta Crystallogr 1952; 5: 802-10; http://dx.doi.org/10.1107/S0365110X52002161
22. Ramachandran GN, Sasisekharan V. Conformations of polypeptides and proteins. Adv Protein Chem 1968; 23: 283-438; PMID:4882249; http://dx.doi.org/10.1016/S0065-3233(08)60402-7
23. Holm L, Sander C. Protein structure comparison by alignment of distance matrices. J Mol Biol 1993; 233:123-38; PMID:8377180; http://dx.doi.org/10.1006/jmbi.1993.1489
24. Nar H, Messerschmidt A, Huber R, van de Kamp M, Canters GW. X-ray crystal structure of the two site-specific mutants His35Gln and His35Leu of azurin from *Pseudomonas aeruginosa*. J Mol Biol 1991; 218: 427-47; PMID:1901363; http://dx.doi.org/10.1016/0022-2836(91)90723-J
25. Nar H, Huber R, Messerschmidt A, Filippou AC, Barth M, Jaquinod M, van de Kamp M, Canters GW. Characterization and crystal structure of zinc azurin, a by-product of heterologous expression in *Escherichia coli* of *Pseudomonas aeruginosa* copper azurin. Eur J Biochem 1992; 205: 1123-9; PMID:1576995; http://dx.doi.org/10.1111/j.1432-1033.1992.tb16881.x
26. Nishikawa K. An overview on natively unfolded proteins. Seibutsu Butsuri 2009; 49: 4-10; http://dx.doi.org/10.2142/biophys.49.004
27. Wright PE, Dyson HJ. Intrinsically unstructured proteins: re-assessing the protein structure-function paradigm. J Mol Biol 1999; 293: 321-31; PMID:10550212; http://dx.doi.org/10.1006/jmbi.1999.3110
28. Daughdrill GW, Hanely LJ, Dahlquist FW. The C-terminal half of the anti-sigma factor FlgM contains a dynamic equilibrium solution structure favoring helical conformations. Biochemistry 1998; 37:1076-82; PMID:9454599; http://dx.doi.org/10.1021/bi971952t
29. Weiss MA, Ellenberger T, Wobbe CR, Lee JP, Harrison SC, Struhl K. Folding transition in the DNA-binding domain of GCN4 on specific binding to DNA. Nature 1990; 347:575-8; PMID:2145515; http://dx.doi.org/10.1038/347575a0
30. Xue B, Dunbrack RL, Williams RW, Dunker AK, Uversky VN. PONDR-FIT: a meta-predictor of intrinsically disordered amino acids. Biochim Biophys Acta 2010; 1804: 996-1010; PMID:20100603; http://dx.doi.org/10.1016/j.bbapap.2010.01.011
31. Ward JJ, Sodhi JS, McGuffin LJ, Buxton BF, Jones DT. Prediction and functional analysis of native disorder in proteins from the three kingdoms of life. J Mol

Biol 2004; 337: 635-45; PMID:15019783; http://dx.doi.org/10.1016/j.jmb.2004.02.002
32. Linding R, Jensen LJ, Diella F, Bork P, Gibson TJ, Russell RB. Protein disorder prediction: implications for structural proteomics. Structure 2003; 11: 1453-9; PMID:14604535; http://dx.doi.org/10.1016/j.str.2003.10.002
33. Hong CS, Yamada T, Fialho AM, Das Gupta TK, Chakrabarty AM. Transport agents for crossing the blood-brain barrier and into brain cancer cells, and methods of use thereof. US patent 2010; 7807183
34. Dutta Ray T, Lewis LA, Gulati S, Rice PA, Ram S. Novel blocking human IgG directed against the pentapeptide repeat motifs of *Neisseria meningitides* Lip/H.8 and Laz lipoproteins. J Immunol 2011; 186: 4881-94; PMID:21402895; http://dx.doi.org/10.4049/jimmunol.1003623
35. Chaudhari A, Fialho AM, Ratner D, Gupta P, Hong CS, Kahali S, Yamada T, Haldar K, Murphy S, Cho W, et al. Azurin, *Plasmodium falciparum* malaria and HIV/AIDS: inhibition of parasitic and viral growth by azurin. Cell Cycle 2006; 5: 1642-8; PMID:16861897; http://dx.doi.org/10.4161/cc.5.15.2992
36. Naguleswaran A, Fialho AM, Chaudhari A, Hong CS, Chakrabarty AM, Sullivan WJ, Jr. Azurin-like protein blocks invasion of *Toxoplasma gondii* through potential interactions with parasite surface antigen SAG1. Antimicrob Agents Chemother 2008; 52: 402-8; PMID:18070964; http://dx.doi.org/10.1128/AAC.01005-07
37. Warso MA, Richards JM, Mehta D, Christov K, Schaeffer C, Rae Bressler L, Yamada T, Majumdar D, Kennedy SA, Beattie CW, et al. A first-in-class, first-in-human phase I trial of p28, a non-HDM2-mediated peptide inhibitor of p53 ubiquitination in patients with advanced solid tumours. Br J Cancer 2013; 108: 2061-70; PMID:23449360; http://dx.doi.org/10.1038/bjc.2013.74
38. Sambrook J, Fritsch EF, Maniatis T. Molecular cloning. A Laboratory Manual, second ed., Cold Spring Harbor Laboratory Press, Cold Spring Harbor, NY. 1989.
39. Laemmli UK. Cleavage of structural proteins during the assembly of the head of bacteriophage T4. Nature 1970; 227: 680-5; PMID:5432063; http://dx.doi.org/10.1038/227680a0
40. Otwinoski Z, Minor W. Processing of X-ray diffraction data collected in oscillation mode. Methods Enzymol 1997; 276: 307-26; http://dx.doi.org/10.1016/S0076-6879(97)76066-X
41. Vagin A, Teplyakov A. Molecular replacement with MOLREP. Acta Crystallogr Sect D Biol Crystallogr 2010; 66: 22-5; PMID:20057045; http://dx.doi.org/10.1107/S0907444909042589
42. Collaborative Computational Project. The CCP4 suite: programs for protein crystallography. Acta Crystallogr Sect D Biol Crystallogr 1994; 50: 760-3; PMID:15299374; http://dx.doi.org/10.1107/S0907444994003112
43. Emsley P, Cowtan K. Coot: model-building tools for molecular graphics. Acta Crystallogr Sect D Biol Crystallogr 2004; 60: 2126-32; PMID:15572765; http://dx.doi.org/10.1107/S0907444904019158
44. Murshudov GN, Vagin AA, Dodson EJ. Refinement of macromolecular structures by the maximum-likelihood method. Acta Crystallogr Sect D Biol Crystallogr 1997; 53: 240-55; PMID:15299926; http://dx.doi.org/10.1107/S0907444996012255
45. Kabsch W. A solution for the best rotation to relate two sets of vectors. Acta Crystallogr Sect A 1976; 32: 922-3; http://dx.doi.org/10.1107/S0567739476001873
46. Laskowski RA, MacArthur MW, Moss DS, Thornton JM. PROCHECK: a program to check the stereochemical quality of protein structures. J Appl Crystallogr 1993; 26: 283-91; http://dx.doi.org/10.1107/S0021889892009944
47. DeLano WL. The PyMOL Molecular Graphics System. DeLano Scientific LLC, San Carlos, CA. 2004
48. Berman HM, Westbrook J, Feng Z, Gilliland G, Bhat TN, Weissig H, Shindyalov IN, Bourne PE. The protein data bank. Nucleic Acids Res 2000; 28: 235-42; PMID:10592235; http://dx.doi.org/10.1093/nar/28.1.235